Visual Neuroscience

ARTICLE

Open Access

https://doi.org/10.48130/vns-0026-0012

Visual Neuroscience **2026**, 43: e021

ChemR23/PTEN suppresses inflammation in retinal Müller cells and retinal ganglion cell damage in diabetic mice

Tao Lv[1], Shilei Sun[1], Zhongfu Zuo[2] and Chuang Feng[3*]

[1] *Department of Ophthalmology, Dandong City First Hospital, Dandong 118000, China*
[2] *Liaoning Key Laboratory of Diabetic Cognitive and Perceptive Dysfunction, Jinzhou Medical University, Jinzhou 121001, China*
[3] *Department of Anatomy, School of Basic Medicine, Jinzhou Medical University, Jinzhou 121001, China*
* Correspondence: fc@jzmu.edu.cn (Feng C)

Abstract

Diabetic retinopathy (DR) is a leading cause of vision impairment, yet the role of chemerin receptor 23 (ChemR23) in its progression remains unclear. This study aimed to explore the function of ChemR23 in modulating Müller cells' activation and injury to retinal ganglion cells (RGCs) in DR. Using 75 *db/db* and 16 wild-type mice divided into eight groups, we assessed ChemR23 expression and its interaction with phosphatase and tensin homolog (PTEN) through molecular docking and surface plasmon resonance. Immunofluorescence confirmed the co-localization of ChemR23 with glutamine synthetase (GS) and PTEN in Müller cells. Histological evaluation revealed retinal thinning and RGCs in 18-week *db/db* mice, accompanied by reduced synaptic markers (SYN, PSD95) and PTEN, alongside elevated glial fibrillary acidic protein, inflammatory cytokines, and phosphorylated protein kinase B (AKT). Activation of ChemR23 with Resolvin E1 (RvE1) or Chemerin 9 (C9) ameliorated these pathological changes. However, the protective effects were abolished by the PTEN inhibitor SF1670. These findings demonstrate that ChemR23 may regulate AKT phosphorylation through its interaction with PTEN, thereby protecting the retinal neurons and suppressing inflammatory responses and Müller cell activation in DR.

Citation: Lv T, Sun S, Zuo Z, Feng C. 2026. ChemR23/PTEN suppresses inflammation in retinal Müller cells and retinal ganglion cell damage in diabetic mice. *Visual Neuroscience* 43: e021 https://doi.org/10.48130/vns-0026-0012

Introduction

Diabetic retinopathy (DR), an extremely prevalent and severe ocular complication[1], is facing mounting challenges in prevention and control because of the increasing incidence of diabetes[2]. The etiology of DR is multifaceted, encompassing various factors where inflammation plays a pivotal role in altering the related structures and functions[3,4]. Studies have correlated the progression of DR with a marked rise in both systemic and ocular inflammatory markers, including elevated concentrations of interleukin (IL)-1β and IL-6[5]. These markers not only exacerbate retinal inflammation but also contribute to vascular and neuronal degradation[6]. The Müller cells stand out as the principal glial cells within the retina, playing an essential role in preserving retinal stability, facilitating neuronal differentiation, and enabling signal transduction[7]. In the context of DR, these cells are activated, leading to a marked upregulation of glial fibrillary acidic protein (GFAP) expression as well as the secretion of a wide array of inflammatory mediators[8,9]. The activation leads to damage in the retinal ganglion cells (RGCs), triggering apoptosis and causing disruptions in the blood–retinal barrier that result in vascular leakage, macular edema, and neovascularization, ultimately resulting in significant retinal injury[10–12]. Consequently, targeting Müller cells with anti-inflammatory interventions could substantially mitigate ocular inflammation and potentially alleviate DR[13].

Chemerin receptor 23 (ChemR23), functions as a G-protein-coupled receptor and is expressed in various cell types, including glial cells and neurons[14–16]. Research involving ChemR23-deficient mice has underscored the receptor's anti-inflammatory effects[17]. Additional *in vitro* studies have shown that the silencing of ChemR23 downregulates the expression of vascular endothelial growth factor (VEGF) and inhibits the migration of rats' primary retinal microvascular endothelial cells in both normoglycemic and hyperglycemic environments, highlighting its crucial involvement in the pathogenesis of DR[18]. However, the exact role of ChemR23 in DR has yet to be completely clarified.

Within the domain of inflammation modulation, Resolvin E1 (RvE1) and chemerin, both naturally occurring agonists of ChemR23, play a vital role[19,20]. RvE1, a derivative of eicosapentaenoic acid and a member of the specialized pro-resolving mediator superfamily[21], plays a significant role in modulating inflammation through its interaction with ChemR23 in myeloid cells, including macrophages, dendritic cells, neutrophils, and natural killer cells. This interaction leads to a reduction in the secretion of tumor necrosis factor (TNF)-α and IL-12 by dendritic cells (DCs)[22]. Chemerin, on the other hand, is an adipokine known for its role in promoting the migration of macrophages and DCs by activating ChemR23 and exhibits both pro- and anti-inflammatory effects[23]. C9, the most biologically active fragment of chemerin, has been identified for its anti-inflammatory capabilities[24]. As the significance of RvE1 and chemerin in metabolic disorders and inflammation becomes increasingly recognized, the complex mechanisms of their shared receptor, ChemR23, need further exploration[25].

This investigation aims to delineate the alterations in ChemR23 expression within the retinas of *db/db* mice and assess the therapeutic effects of RvE1 and C9 in modulating ChemR23's activity on DR. Moreover, we explore the potential mechanisms through which ChemR23 signaling could attenuate inflammation, and Müller cell activation and reduce damage to the RGCs.

Materials and methods

Animals and groups

From Charles River, Japan, we obtained 75 male BKS-Lepr/*db/db*/JOrlRj mice (six weeks old) that were defective in

the leptin receptor (*db/db*) and 16 gender-matched wild-type (WT, C57BLKS/JGpt) mice. The mice were housed in a designated pathogen-free area at Jinzhou Medical University. They were subjected to a 12-h light/dark cycle, kept at 20–25 °C and given free access to food and drink. After adjusting to the environment for 3 d, WT and *db/db* mice were divided into different groups for research. These groups included WT, *db/db* at 8 weeks (db 8w) (n = 4 mice, 8 eyeballs), db at 18 weeks (db 18w) (n = 19 mice, 38 eyeballs), and db at 26 weeks (db 26w) (n = 4 mice, 8 eyeballs), as well as groups that received treatments with *db/db* + Resolvin E1 (RvE1) (n = 12 mice, 24 eyeballs), *db/db* + Chemerin 9 (C9) (n = 12 mice, 24 eyeballs), *db/db* + RvE1 + SF1670 (n = 12 mice, 24 eyeballs), and *db/db* + C9 + SF1670 (n = 12 mice, 24 eyeballs). All procedures involving animals were carried out in accordance with the standards set by the Vision and Ophthalmology Research Association and were approved by the Animal Experiment Ethics Committee of Jinzhou Medical University on April 2, 2023 (No. 2023040201).

Drug administration

Just before injection, RvE1 (item #10007848, Cayman Chemical) was reconstituted in sterile phosphate-buffered saline (PBS) after being evaporated under a mild nitrogen stream. Chemerin 9 (Item #7117, Tocris Bioscience) was dissolved directly in sterile PBS. For 8 weeks, the subjects were given intraperitoneal injections of either RvE1 (6 μg/kg) or C9 (60 μg/kg) once daily, whereas the control groups received the same volume of PBS[26]. Mice were injected intraperitoneally with the PTEN inhibitor SF1670 (SML0684, Sigma-Aldrich) (3 mg/kg diluted in 50 μL 0.4% methylcellulose) daily for 8 weeks[27].

Tissue collection

For the time-course study, *db/db* mice were reared to 8, 18, and 26 weeks of age. Mice from the WT, db 8w, db 18w, and db 26w groups (n = 4 mice, 8 eyeballs per group) were euthanized by an intraperitoneal injection of a 10 g/L pentobarbital sodium solution, followed by transcardial perfusion with physiological saline. Eyeballs were promptly enucleated and immersed in physiological saline. Under a dissection microscope, the vitreous body was removed, and the retina was carefully dissected. After blotting away excess moisture, retinal tissues were placed in Eppendorf tubes and stored at −80°C for subsequent molecular analyses. Five retinas per group were allocated for quantitative real-time polymerase chain reaction (qRT-PCR), and three per group for Western blot (WB) analysis.

Following 8 weeks of intraperitoneal intervention with RvE1, C9, and/or SF1670, *db/db* mice were processed for tissue collection. All groups except the *db/db* 18w group comprised 12 mice (24 eyeballs); the *db/db* 18w group consisted of 15 mice (30 eyeballs). Mice were euthanized and perfused as described above. Retinas were dissected and stored at −80 °C for the following assays: WB (four retinas per group), enzyme-linked immunosorbent assay (ELISA) (five retinas per group), and surface plasmon resonance (SPR) analysis (five retinas per group).

The remaining eyeballs were processed for histology. Under a dissection microscope, a circumferential incision was made along the corneal limbus, and the vitreous body was removed to obtain eye cups with the retina intact. These eye cups were fixed in a specialized ocular fixation solution. From each group, five eye cups were allocated for hematoxylin and eosin (H&E) staining and another five for immunohistochemical staining. Additionally, six eyeballs from the *db/db* 18w group were reserved for immunofluorescence staining.

H&E staining

Before being embedded in paraffin and dehydrated in alcohol, the eyeballs were fixated in a specific eyeball fixation solution at 4 °C for 48 h to facilitate histological studies. Hematoxylin and eosin were applied to 4-micron sections that had been made using a paraffin slicer. The sections were dewaxed, rehydrated, and left at room temperature for staining. Following the staining process, the slices were rinsed, dried, and finally mounted using neutral glue. Photographs were captured using an inverted fluorescence microscope (Olympus, Japan) at the region 300 μm posterior to the optic nerve. The distance from the retinal ganglion cell layer to the outer nuclear layer was measured as an indicator of relative retinal thickness (compared with the WT group). Additionally, the number of RGCs in the retinal ganglion cell layer was quantified for each field of view.

Immunofluorescence

Retinal sections were cut (10 μm thickness), frozen, and incubated for 2 h at room temperature with primary rabbit monoclonal antibodies targeting glutamine synthetase (GS) (ab176562), PTEN (ab170941), and ChemR23 (ab306554), all obtained from Abcam PLC, and diluted 1:200. After the primary antibody was incubated, the sections were rinsed with PBS. Then they were incubated for 30 min with Alexa Fluor 488 (ab302584) and 647 (ab300751) secondary antibodies, both diluted 1:400 in PBS. Sections were preserved with an anti-quenching agent and subsequently visualized and analyzed using an Olympus fluorescence microscope.

Immunohistochemistry

Before being incubated with 3% H_2O_2 to inhibit endogenous peroxidase activity, retinal slices (10 μm thickness) fixed in paraffin underwent dewaxing, rehydration, and PBS washing. First, 3% bovine serum albumin was used for blocking, then a GFAP antibody (Abcam, Cambridge, United Kingdom) was diluted to 1:1,500 and incubated overnight at 4 °C. After that, there were three washes with PBS before the sections were incubated with a secondary antibody coupled with horseradish peroxidase (HRP) (K5007, DAKO, Glostrup, Denmark) for 50 min. Following further washing, the sections were subjected to 3,3'-diaminobenzidine tetrahydrochloride treatment for about 1 min. Hematoxylin was then used as a counterstain. Subsequently, the sections were dehydrated, cleared, and mounted with synthetic glue. The density of GFAP-positive cells was quantified using ImageJ across three representative slices from each group.

ELISA

Blood was collected from mouse eyeballs, then 10 μL of serum was taken and added to each well. The absorbance of each sample was recorded at 450 nm, and the levels of IL-1β, IL-18, IL-6, and TNF-α in the supernatant were obtained according to the instructions of the ELISA kit (TNF-α: ab208348; IL-6: ab222503; IL-1β: ab197742; IL-18: ab216165).

qRT-PCR

Three retinas were pooled for RNA extraction in each group. Total RNA was isolated using Trizol reagent (Sigma-Aldrich) in combination with a tissue homogenizer (Kinematica Polytron, ThermoFisher). RNA purification was achieved through liquid–liquid extraction, and the aqueous phase was collected for further isolation and purification. Reverse transcription of RNA to cDNA was performed using the

HiScript Q RT SuperMix for qRT-PCR (Vazyme, China). qRT-PCR was carried out using FastStart Universal SYBR Green Master Mix (Roche). The relative mRNA expression levels were normalized to β-actin using the $2^{-\Delta\Delta CT}$ method. The mouse primers for ChemR23 were forward: 5'-ATGGAGTACG ACGCTTACAACG-3' and reverse: 5'-GGTG-GCGATGACAATCACCA-3'; those for GAPDH were forward: 5'-TGCATCCTGCACCACCAACTGC-3' and reverse: 5'-ACAGCCTTG-GCAGCACCAGTGG-3'.

Western blotting

After retinal detachment, all proteins were extracted using a tissue lysate (Beyotime, China). We used the BCA Protein Analysis Kit (Epizyme, China) to identify the protein concentration. Polyvinylidene fluoride membranes, which were crosslinked with 5% skim milk, were used for protein separation after sodium dodecyl sulfate-polyacrylamide gel electrophoresis. Primary antibodies specific to ChemR23 (A15237), synaptophysin (SYN) (A6344), PSD95 (A7889), PTEN (ab170941), AKT (A17909), and p-AKT (AP0140) were mixed with β-actin (1:1,000, 3,700, CST, USA) and incubated with the membranes overnight at 4 °C. Following a tris-buffered saline with tween 20 (TBS-T) wash, the membranes were incubated at 37 °C for 1 h with HRP-conjugated anti-rabbit Immunoglobulin G (IgG) (GB23303, 1:1000, Servicebio). Proteins were visualized using a chemiluminescent substrate (Yeasen, Shanghai, China), and band intensities were normalized against β-actin. The gray values of the protein bands were analyzed using ImageJ software, and the relative expression results of the target protein were calculated (the gray value of the target protein was compared with the average gray value of the internal reference protein).

Protein–protein interaction network

The STRING database was utilized to investigate potential protein–protein interactions among Chemerin, ChemR23, and PTEN, considering only experimentally validated interactions with a combined score of 0.4 or higher as significant.

Molecular docking

Structural files were obtained from the Protein Data Bank (PDB): ChemR23 (PDB: 7YKD) and PTEN (PDB: 1D5R).

SPR analysis

To quantify the affinity, Creative Biolab used a Biacore T200 system, manufactured by GE Healthcare Life Sciences. A solution comprising 400 mM 1-ethyl-3-(3-dimethylaminopropyl) carbodiimide (EDC) and 100 mM N-hydroxysuccinimide (NHS) was used to activate the surface of the CM5 sensor chip first. After that, the chip's surface was linked to a PTEN solution (20 μg/mL) in a sodium acetate buffer (pH 4.5) at 10 μL/min for 30 s. After 30 min of treatment with 1 M ethanolamine (pH 8.5), blocking was accomplished. The system was equilibrated with PBS-P buffer for a minimum of 2 h to stabilize the baseline. For real-time interaction analysis, PTEN was injected in various concentrations across the sensor chip at 30 μL/min for 120 s, and 900 s thereafter. The surface was regenerated using 0.1 mM NaOH for 10 s. Interaction monitoring (with a sensorgram) was performed at 25 °C, and adjustments were made using the reference surface data. We used BIAcore T200 evaluation software, version 3.1, to fit curves and obtain kinetic parameters such the association constant (Ka), the dissociation constant (Kd), and the equilibrium dissociation constant (KD = Kd/Ka).

Statistical analysis

A standard error of the mean (SEM) format is used for presenting the data. Statistical analysis was performed using SPSS, version 23.0. All data followed a normal distribution. We used one-way analysis of variance (ANOVA) followed by Tukey's post hoc test to find statistically significant differences when there were more than three groups in our analysis. A p-value < 0.05 was considered to be statistically significant. Detailed graphical presentations of the results were processed using GraphPad Prism, version 9, with ** $p < 0.01$ indicating significant differences.

Results

Expression pattern of ChemR23

To investigate the expression dynamics of ChemR23 in DR, qRT-PCR and WB analyses were conducted on the retinas of diabetic mice aged 8, 18, and 26 weeks. As depicted in Fig. 1a–c, both mRNA and levels of ChemR23 were reduced at 18 and 26 weeks ($p < 0.01$), with no notable changes observed at 8 weeks. Consequently, 18-week-old *db/db* mice were selected for subsequent experiments. To further investigate ChemR23 expression in nerve glial cells, retinal sections from *db/db* mice were subjected to ChemR23/GS double immunofluorescence staining. The analysis revealed the predominant expression of ChemR23 in Müller cells (Fig. 1d). These findings suggest a potential link between DR and ChemR23 signal transduction.

ChemR23 activation by RvE1 or C9 attenuated damage to RGCs

Administering the ChemR23 agonists RvE1 or C9 to 18-week-old *db/db* mice for 8 weeks allowed us to assess the impact of activating ChemR23 on RGCs in diabetic settings. Although RvE1 and C9 treatments significantly reduced fasting blood glucose levels in *db/db* mice ($p < 0.01$) (Fig. 2c), body weight showed only a nonsignificant increasing trend (Fig. 2d). H&E staining of retinal sections revealed neuronal deterioration and necrotic RGCs in untreated *db/db* mice. In contrast, treatments with RvE1 and C9 appeared to mitigate these deleterious changes (Fig. 2a). Semiquantitative assessments indicated a decrease in both retinal thickness and RGC counts in the *db/db* group ($p < 0.01$). Treatment with either RvE1 or C9 significantly improved the histopathological conditions and increased retinal thickness in *db/db* mice ($p < 0.01$) (Fig. 2b, e). Furthermore, to determine whether the activation of ChemR23 through RvE1 or C9 could enhance synaptic plasticity and axon regeneration in diabetic retinal neurons, WB was used to monitor changes in the proteins related to these processes, specifically SYN, and PSD95. The levels of these proteins' expression, which were significantly lower in *db/db* animals ($p < 0.01$), significantly increased after RvE1 or C9 therapy ($p < 0.05$) (Fig. 2f, g). These findings point to possible therapeutic avenues for reducing neuronal loss in DR, as activation of ChemR23 by RvE1 or C9 successfully decreases neuronal damage in diabetic mice.

ChemR23 activation by RvE1 or C9 mitigated inflammatory responses and Müller cell activation

To investigate whether ChemR23 activation regulates inflammatory responses and Müller cell activation, we initially analyzed GFAP expression in the retinal tissues of *db/db* mice using

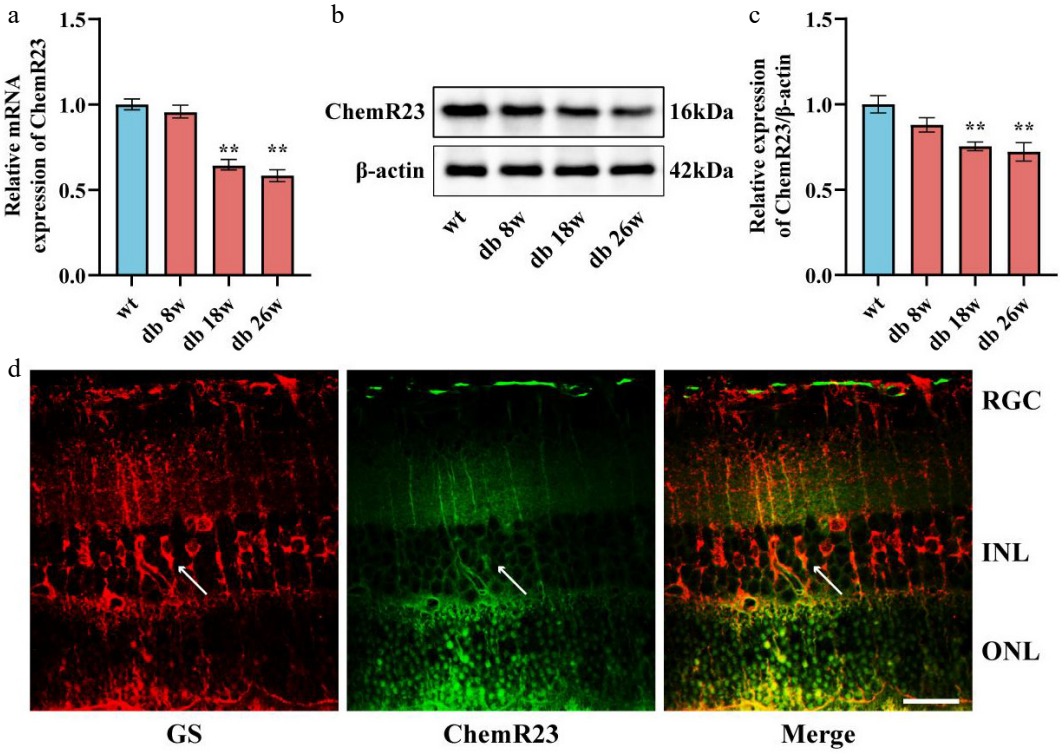

Fig. 1 Expression pattern of ChemR23. (a) qRT-PCR analysis of ChemR23 in the retina of *db/db* mice aged 8, 18, and 26 weeks. For each group, $n = 5$. (b, c) Representative Western blot bands and semiquantitative analysis of ChemR23 in the retinas of *db/db* mice aged 8, 18, and 26 weeks. For each group, $n = 3$. Data are expressed as the average value ± SEM. $^{**}p < 0.01$ vs WT. (d) Combined immunofluorescence images of the representative ChemR23 and GS in the retina of *db/db* mice aged 18 weeks. The white arrows indicate the coexpression of GS and ChemR23. Scale: 50 μm. For each group, $n = 3$.

immunohistochemistry. Significant Müller cell activation was noted in the retinas of *db/db* mice, evidenced by extensive GFAP-positive staining from the nerve fiber layer to the outer nuclear layer in a columnar configuration (Fig. 3a, b). This abnormal GFAP expression, indicative of Müller cell activation, was significantly reduced following treatment with RvE1 or C9. ELISA was subsequently used to measure the levels of proinflammatory cytokines related to Müller cell activation. These cytokines were significantly elevated in the retinas of *db/db* mice ($p < 0.01$) but were notably decreased in *db/db* mice treated with RvE1 or C9 ($p < 0.05$) (Fig. 3c–f). In conclusion, ChemR23 activation by RvE1 and C9 effectively reduces inflammatory responses and Müller cell activation in diabetic mice.

ChemR23 interacts with PTEN

To elucidate the potential role of ChemR23 (also known as CMKLR1) in modulating Müller cell activation and RGC injury, we established a PPI network utilizing the STRING database. This network explored the interactions of ChemR23 with key signaling molecules including PTEN. As shown in Fig. 4a, this network revealed a direct interaction between ChemR23 and PTEN, suggesting a functional correlation. To confirm this interaction, a molecular docking analysis of ChemR23 with PTEN was performed. Figure 4c displays the molecular docking model, which simulates the spatial binding of the two molecules. To further confirm the direct interaction between ChemR23 and PTEN, SPR analysis was carried out. The SPR results (Fig. 4b) demonstrated a significant dose-dependent interaction between ChemR23 and PTEN, with an increased ChemR23 concentration enhancing the binding signal. This finding validated the molecular docking predictions and supported the interaction of ChemR23 with PTEN under physiological conditions. Additionally, to examine their colocalization *in vivo*, immunofluorescence was used to analyze retinal tissue from the mice. The results confirmed significant coexpression of ChemR23 and PTEN in the retina, further supporting their potential synergistic role in retinal function (Fig. 4d). In summary, the interaction between ChemR23 and PTEN has been preliminarily demonstrated.

ChemR23 activation may depend on its interaction with PTEN to reduce damage to RGCs

Considering the significant protective impact of ChemR23 activation observed in the retina of *db/db* mice and the initial confirmation of ChemR23's interaction with PTEN, we investigated whether ChemR23 alleviated damage to RGCs through this interaction. SF1670, a selective PTEN inhibitor, was administered to *db/db* mice treated with RvE1 or C9, activators of ChemR23. H&E staining analysis revealed that SF1670 significantly reduced the therapeutic protective effects of RvE1 and C9 against damage to RGCs, suggesting that PTEN inhibition might disrupt the beneficial effects of ChemR23 activation (Fig. 5a). Additionally, PTEN inhibition led to decreased retinal thickness and a reduction in RGC numbers in *db/db* mice ($p < 0.05$) (Fig. 5b, c). WB analysis showed that the expression levels of SYN and PSD95 were significantly lower in mice treated with *db/db* + RvE1 + SF1670 or *db/db* + C9 + SF1670 compared with those treated with RvE1 or C9 alone ($p < 0.05$) (Fig. 5d, e). These findings suggest that ChemR23 activation may depend on its interaction with PTEN to mitigate damage to the RGCs and promote axon regeneration and synaptic plasticity in the retina.

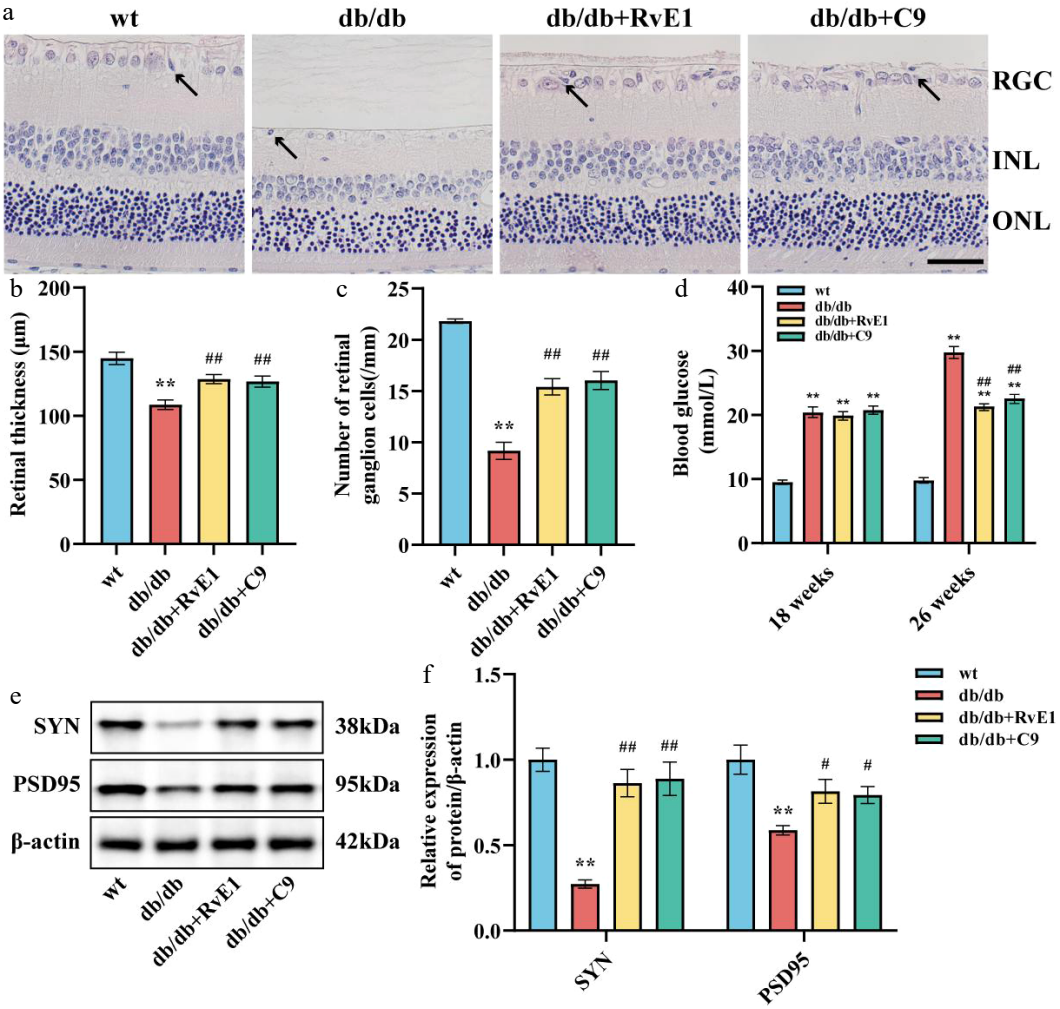

Fig. 2 ChemR23 activation by RvE1 or C9 attenuated damage to RGCs. (a) Representative H&E staining of the retina in *db/db* mice aged 18 weeks after intraperitoneal injection treatment with RvE1 or C9 for 8 weeks. Black arrows indicate necrotic RGCs. Scale: 50 μm. For each group, $n = 5$. (b) and (e) Semiquantitative analysis of retinal thickness and the number of RGCs. (c) Comparison of fasting blood glucose in each group of mice. (d) Comparison of body weight in each group of mice. (f) SYN and PSD95 are representative Western blot bands. For each group, $n = 4$. (g) Semiquantitative analysis of SYN, and PSD95. For each group, $n = 4$. Data are expressed as the average value ± SEM. $^{**}p < 0.01$ vs WT. $^{\#}p < 0.05$, $^{\#\#}p < 0.01$ vs *db/db*.

ChemR23 activation may depend on its interaction with PTEN to attenuate inflammatory responses and Müller cell activation

Next, we examined whether ChemR23 activation reduces inflammatory responses and Müller cell activation through its interaction with PTEN. SF1670 significantly diminished the inhibitory effect of RvE1 and C9 on Müller cell activation (Fig. 6a, b). The ELISA results indicated that IL-1β, IL-6, IL-18, and TNF-α levels were significantly higher in the retinas of mice treated with RvE1 + SF1670 or C9 + SF1670 compared with those treated with RvE1 or C9 alone ($p < 0.05$) (Fig. 6c–f). These results confirm that ChemR23 activation attenuates inflammatory responses and Müller cell activation by interacting with PTEN.

ChemR23 rescues DR by activating AKT after interacting with PTEN

Research underscores the critical function of the AKT pathway in promoting inflammation, with PTEN acting as a negative regulator by converting phosphatidylinositol (3,4,5)-trisphosphate (PI (3,4,5) P3) into phosphatidylinositol (4,5)-bisphosphate (PIP2), thereby exerting anti-inflammatory effects. WB analysis was utilized to measure the relative expression of p-AKT and PTEN in the retinas of all experimental groups (Fig. 7a). In contrast to the *db/db* group, mice treated with RvE1 and C9 showed a marked reduction in AKT phosphorylation and an increase in PTEN expression ($p < 0.01$). However, these effects were reversed upon treatment with the PTEN inhibitor SF1670 ($p < 0.01$). Moreover, compared with treatments with RvE1 or C9 alone, the combination of these agents with SF1670 led to reduced PTEN levels and elevated p-AKT levels ($p < 0.05$) (Fig. 7b, c). This indicates that SF1670 enhances AKT activity by inhibiting PTEN's function and its negative regulation of p-AKT, potentially diminishing the protective effect of RvE1 and C9 in DR through an intensified inflammatory response driven by increased p-AKT.

Discussion

The present study focused on the activation of ChemR23 and its possible protective mechanisms in relation to DR in *db/db* mice. Initially, a significant decrease in ChemR23 expression was noted in

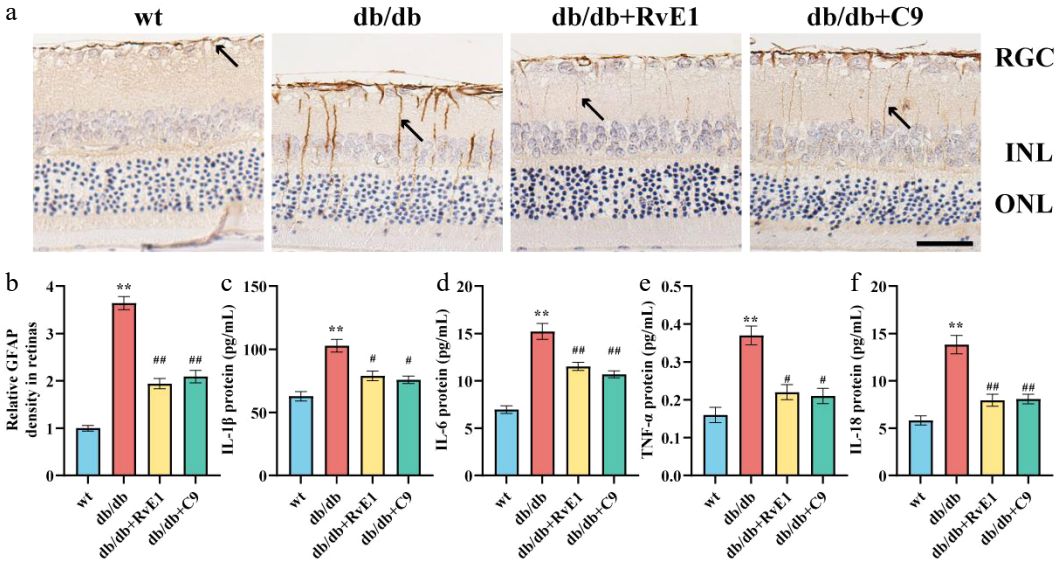

Fig. 3 ChemR23 activation by RvE1 or C9 mitigated inflammatory responses and Müller cell activation. (a) Representative immunohistochemical staining of retinal GFAP in *db/db* mice aged 18 weeks after intraperitoneal injection treatment with RvE1 or C9 for 8 weeks. The black arrow indicates the positive expression of GFAP. Scale: 50 μm. For each group, $n = 5$. (b) Quantitative analysis of the relative density of retinal GFAP. For each group, $n = 5$. Data are expressed as the average value ± SEM. ** $p < 0.01$ vs WT. $^{\#\#}$ $p < 0.01$ vs *db/db*. (c–f) The protein levels of IL-1β, IL-6, IL-18, and TNF-α in the retina of *db/db* mice aged 18 weeks treated with RvE1 or C9 via intraperitoneal injection for 8 weeks determined by ELISA. For each group, $n = 5$. Data are expressed as the average value ± SEM. ** $p < 0.01$ vs WT. $^{\#}$ $p < 0.05$, $^{\#\#}$ $p < 0.01$, vs *db/db*.

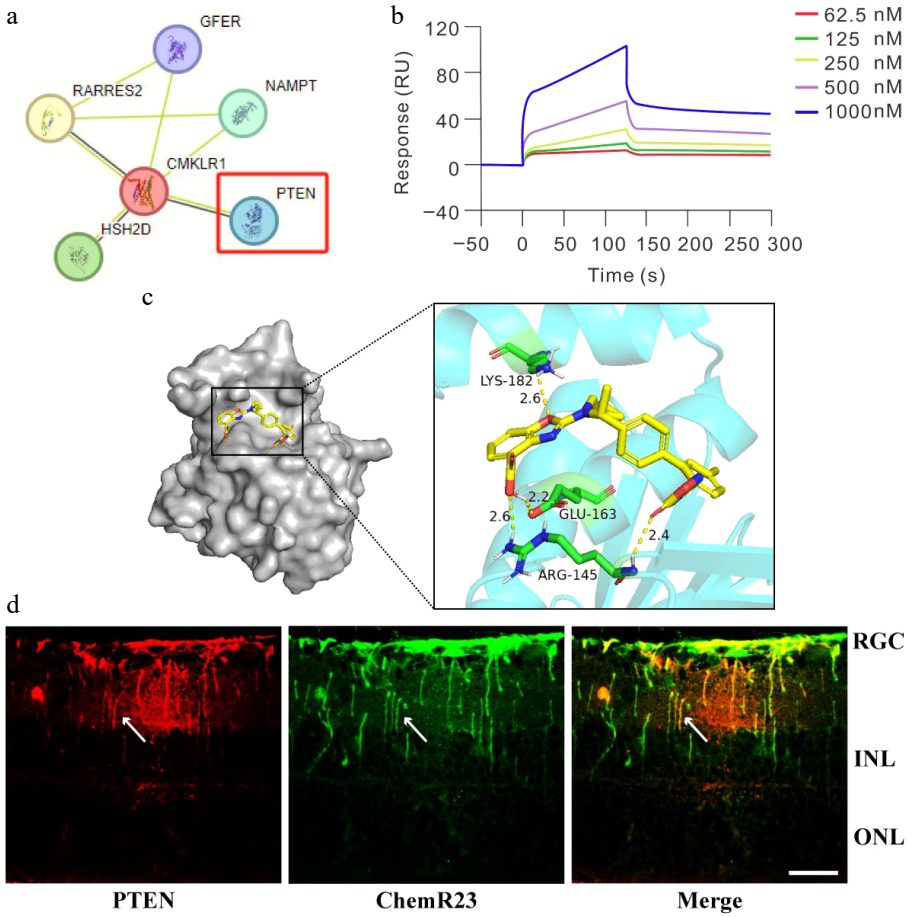

Fig. 4 ChemR23 interacts with PTEN in the retinas of diabetic mice. (a) The PPI network of ChemR23 and PTEN. (b) SPR analysis of the binding of ChemR23 and PTEN. PTEN is fixed on the CM5 BIAcore chip and interacts with ChemR23 at the specified concentration. (c) Diagram of the molecular docking model. The cyan molecules represent ChemR23, the yellow molecules represent PTEN, and the green molecules represent the amino acids that combine PTEN with ChemR23, namely lysine-182, glutamate-163 and arginine-145. (d) Immunofluorescence colocalization of ChemR23 and PTEN in the retina of *db/db* mice aged 18 weeks. The white arrows indicate the coexpression of PTEN and ChemR23. Scale: 50 μm. For each group, $n = 3$.

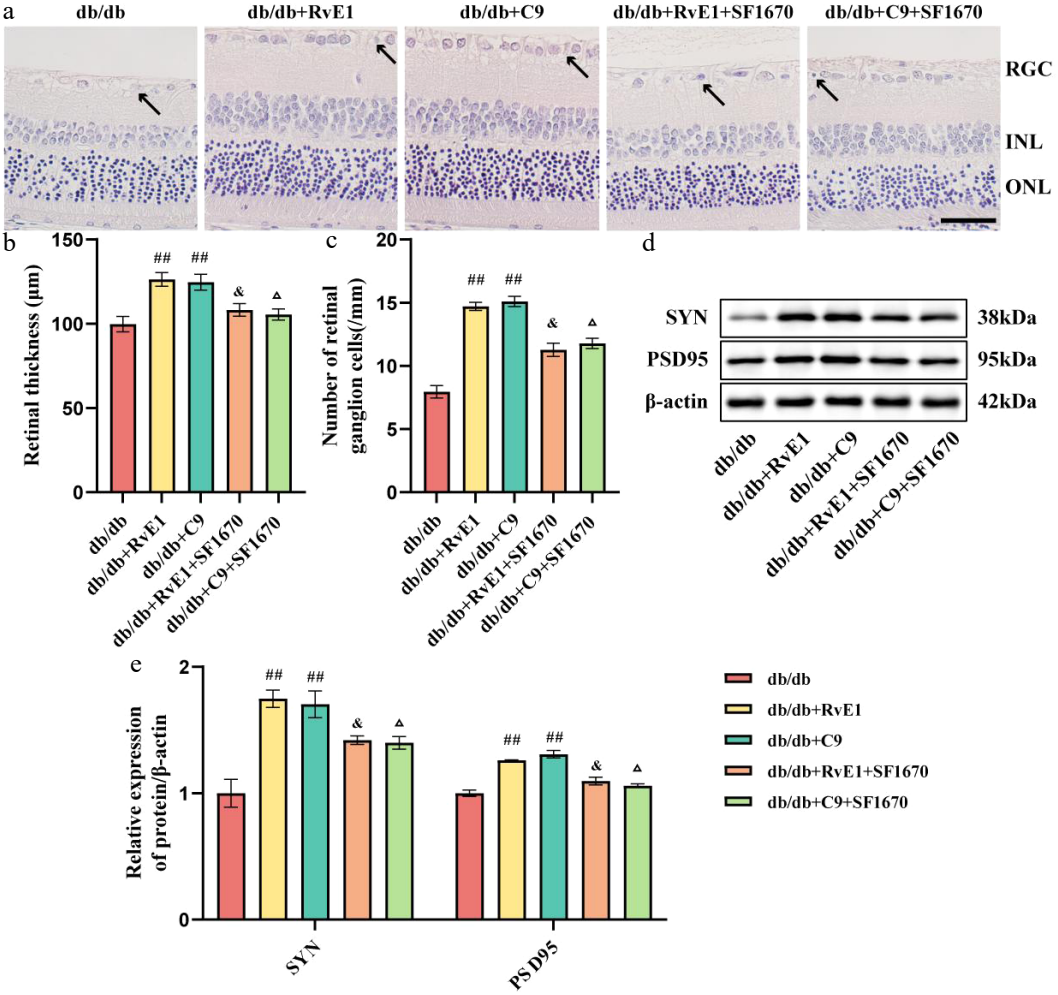

Fig. 5 ChemR23 activation depend on its interaction with PTEN to reduce damage to RGCs. (a) Representative H&E staining of the retina of *db/db* mice aged 18 weeks after intraperitoneal injection treatment with RvE1 or C9 and SF1670 (selective inhibitors of PTEN) for 8 weeks. Black arrows indicate necrotic RGCs. Scale: 50 μm. For each group, $n = 5$. (b, c) Semiquantitative analysis of retinal thickness and the number of RGCs. For each group, $n = 5$. Data are expressed as the average value ± SEM. $^{\#\#}$ $p < 0.01$ vs *db/db*. $^{\&}$ $p < 0.05$ vs *db/db* + RvE1. $^{\Delta}$ $p < 0.05$ vs *db/db* + C9. (d, e) Representative Western blot bands and semiquantitative analysis of SYN and PSD95. For each group, $n = 4$. Data are expressed as the average value ± SEM. $^{\#\#}$ $p < 0.01$ vs *db/db*. $^{\&}$ $p < 0.05$ vs *db/db* + RvE1. $^{\Delta}$ $p < 0.05$ vs *db/db* + C9.

the retinas of these mice. Subsequent treatments with the ChemR23 agonists RvE1 or C9, successfully mitigated neuronal damage in the retina, reduced Müller cell activation, and enhanced axonal growth as well as synaptic plasticity in the retinal neurons. We also demonstrated a clear interaction between ChemR23 and PTEN, with PTEN binding to ChemR23 in a highly efficient and dose-dependent manner. Additionally, when PTEN inhibitors were administered, the protective effect of ChemR23 activation was significantly diminished and AKT phosphorylation was inhibited. Our findings indicate that ChemR23 may influence AKT phosphorylation via its interaction with PTEN, contributing to the protection of retinal neurons and reduced Müller cell activation. Thus, our findings suggest that ChemR23 may regulate AKT phosphorylation through its interaction with PTEN, thereby potentially protecting retinal neurons and suppressing inflammation in DR. This discovery not only advances our understanding of ChemR23's protective role in DR but also lays the groundwork for potential new therapeutic approaches targeting this mechanism.

Recent research has highlighted the critical role of ChemR23 as a therapeutic target in diabetes and its associated complications. As a chemotactic receptor, ChemR23's biological effects vary with the specific ligand bound[28,29]. For example, research conducted by Jun et al. has demonstrated that chemerin increases the expression of intercellular adhesion molecule-1 through a ChemR23-dependent mechanism, thereby facilitating angiogenesis[18]. Conversely, Shang et al. identified the chemerin–ChemR23 axis as an inflammatory inducer contributing to glomerular endothelial injury and increased expression of inflammatory markers in *db/db* mice[30]. However, C9, a cleavage product of chemerin, exhibits a contrasting role[31]. Moreover, C9 has demonstrated potential in mitigating oxidative stress and NLRP3 inflammasome activation in the hippocampus of mice with Type 1 diabetes induced by streptozotocin (STZ), as well as in *db/db* mice, effectively reducing cognitive impairment[32]. Additionally, the interaction between RvE1 and ChemR23 significantly reduced the neuronal pyroptosis induced by the NLRP3 inflammasome, preserving hippocampal neurons and synapses, thereby improving the cognitive deficits caused by chronic cerebral hypoperfusion[26]. Zhang et al.'s study also supports the importance of ChemR23 in diabetes and its complications, finding that ChemR23 expression in hippocampal tissue was markedly reduced in *db/db* and STZ-induced diabetic mice[32]. In this study, chronic activation of ChemR23 through RvE1 or C9 was found to inhibit

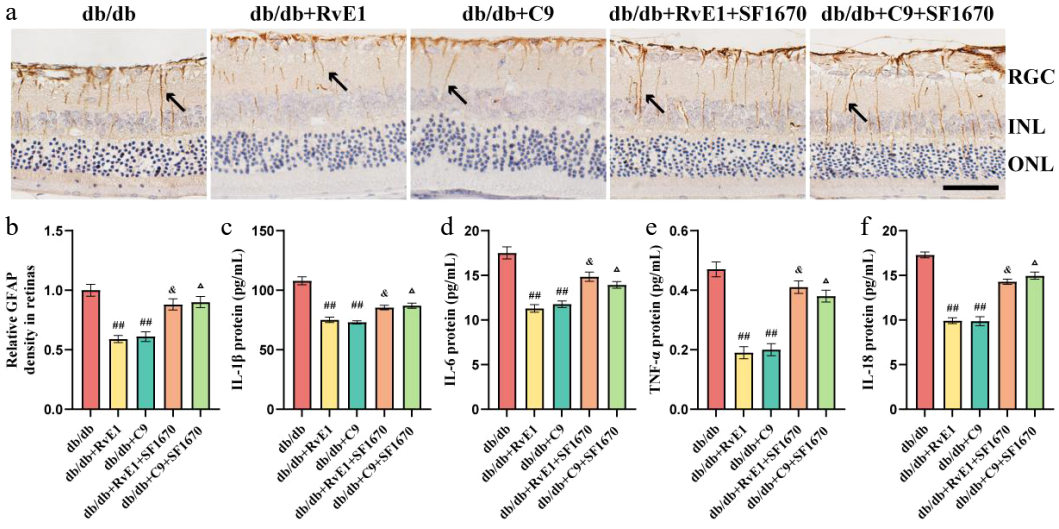

Fig. 6 ChemR23 activation may depend on its interaction with PTEN to attenuate inflammatory responses and Müller cell activation. (a) Representative immunohistochemical staining of retinal GFAP in *db/db* mice aged 18 weeks after intraperitoneal injection treatment with RvE1 or C9 and SF1670 for 8 weeks. The black arrow indicates positive expression of GFAP. Scale: 50 μm. For each group, $n = 5$. (b) Quantitative analysis of the relative density of retinal GFAP. For each group, $n = 5$. Data are expressed as the average value ± SEM. $^{\#\#}p < 0.01$ vs *db/db*. $^{\&}p < 0.05$ vs *db/db* + RvE1. $^{\Delta}p < 0.05$ vs *db/db* + C9. (c–f) The protein levels of IL-1β, IL-6, IL-18, and TNF-α in the retina of *db/db* mice aged 18 weeks after intraperitoneal injection treatment with RvE1 or C9 and SF1670 for 8 weeks were detected by ELISA. For each group, $n = 5$. Data are expressed as the average value ± SEM. $^{\#\#}p < 0.01$ vs *db/db*. $^{\&}p < 0.05$ vs *db/db* + RvE1. $^{\Delta}p < 0.05$ vs *db/db* + C9.

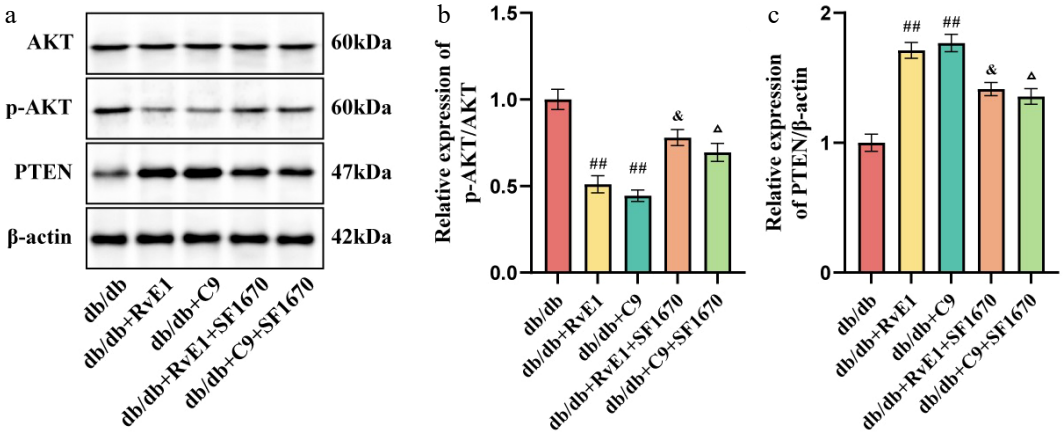

Fig. 7 ChemR23 rescues DR by activating AKT after interacting with PTEN. (a) Representative WB bands of p-AKT/AKT and PTEN/β-actin in the retina of *db/db* mice aged 18 weeks after intraperitoneal injection treatment with RvE1 or C9 and SF1670 for 8 weeks. (b, c) Semiquantitative analysis of p-AKT/AKT and PTEN/β-actin in the retina of *db/db* mice after treatment with RvE1 or C9 and SF1670. For each group, $n = 4$. Data are expressed as the average value ± SEM. $^{\#\#}p < 0.01$vs *db/db*. $^{\&}p < 0.05$ vs *db/db* + RvE1. $^{\Delta}p < 0.05$ vs *db/db* + C9.

inflammatory responses and Müller cell activation in diabetic mice. The findings indicated that by 18 weeks, there was a significant reduction in both ChemR23 mRNA and protein levels within the retinas of *db/db* mice. Importantly, the activation of ChemR23 by RvE1 or C9 led to a notable decrease in retinal neuronal injury and the related inflammatory reactions.

It is widely recognized that synaptic plasticity in the retinal neurons is critical for preserving normal retinal function. Synaptic plasticity involves the dynamic adjustment of synaptic structure and function. SYN, the first successfully cloned synaptic vesicle protein, has long served as a key marker in studying synaptic distribution and function, which are essential for the normal functioning of retinal neurons[33]. Recent studies have demonstrated that activation of the renin–angiotensin system significantly reduces SYN protein levels in the retina of C57BL/6 mice, leading to neuronal dysfunction[34]. A similar decrease in SYN has also been observed in *db/db* diabetic mice and STZ-induced diabetic rat retinas[35,36]. In a study of alloxan-induced diabetic mice, disruptions in the retinal hierarchy were noted, along with upregulation of GFAP, TNF-α, and IL-6[37]. These findings align with ours. In our *db/db* diabetic mouse model, we observed damage to the RGCs accompanied by significant reductions in the expression of synapse-related proteins such as SYN and PSD95, illustrating a strong link between retinal neuron damage and impaired synaptic plasticity in diabetes. Importantly, we also found that synaptic damage was significantly ameliorated by activating ChemR23 with RvE1 or C9.

DR is closely associated with the activation of Müller cells, which are marked by increased expression of GFAP[38]. These cells are instrumental in producing VEGF, a critical factor driving retinal inflammation, neovascularization, and vascular leakage, which are central to the pathological development of DR[39]. As the primary glial cells in the retina, Müller cells also convert glutamate into glutamine via GS, which is essential for clearing glutamate and preventing neurotoxic damage[40]. We observed the colocalization

of ChemR23 and GS in Müller cells, indicating the predominant expression of ChemR23 in these cells. Further investigations revealed that activating ChemR23 markedly reduced GFAP expression, suppressing Müller cell activation. Additionally, as DR progresses, activated Müller cells release a significant number of inflammatory factors, contributing to a chronic inflammatory environment and exacerbating the retinal inflammatory response[41]. Notably, our study also showed that activating ChemR23 significantly reduces the secretion of these inflammatory factors.

The molecular mechanisms underlying ChemR23 signaling in DR merit further exploration. In liver cancer cells, chemerin has been shown to enhance PTEN activity by interrupting its direct interaction with CMKLR1, leading to its ubiquitination and subsequent degradation[42]. Another study reported the upregulation of PTEN transcription mediated by chemokines in prostate and sarcoma cell lines[43]. Additionally, researchers found that chemerin induced endothelial cell apoptosis and vascular regression by activating PTEN and inhibiting the phosphoinositide 3-kinase (PI3K)/AKT pathway[44]. These findings prompted us to explore a new link between ChemR23 and PTEN. This study is the first to reveal the efficient and stable binding between ChemR23 and PTEN. Further research showed that when SF1670 was used to inhibit PTEN activity, ChemR23 did not provide the expected protective effects against DR, even when activated. This discovery not only deepens our understanding of the ChemR23–PTEN interaction mechanism but also highlights the crucial role of PTEN in the ChemR23-mediated pathway.

Although our work has established a direct interaction between ChemR23 and PTEN in DR, the downstream molecular consequences of this interaction on PTEN's function require further clarification. Previous studies have consistently highlighted that PTEN acts as a critical negative regulator of the PI3K/AKT pathway by exerting its tumor-suppressive effects through its phosphatase activity, which dephosphorylates PIP3 to PIP2, thereby opposing PI3K activity[45]. It is important to note that a decrease in PTEN activity may lead to prolonged activation of the PI3K/AKT pathway, which can affect the phenotypic alterations observed in podocytes in hyperglycemic environments[46]. In the early stages of DR, the hyperglycemic conditions can notably inhibit the AKT signaling pathway. This suppression may occur through increased oxidative stress or reduced expression of growth factors, leading to retinal cell apoptosis and the development of microvascular complications. However, as DR progresses, the VEGF/PI3K/AKT cascade becomes markedly active because of compensatory angiogenesis, leading to enhanced levels of AKT phosphorylation[47]. In this study, elevated levels of p-AKT were observed in the retinal tissues of *db/db* diabetic mice. Notably, activation of ChemR23 was associated with reduced levels of p-AKT, suggesting a modulatory role of this receptor in the signaling pathways involved in DR. Conversely, inhibition of PTEN with inhibitors caused an increase in p-AKT levels, further supporting the negative regulatory role of PTEN in thePI3K/AKT pathway and suggesting that ChemR23's regulation of AKT activity may be partially dependent on the functional status of PTEN. One potential avenue through which ChemR23 may modulate PTEN activity is by affecting its subcellular localization. PTEN's ability to access and dephosphorylate PIP3 at the plasma membrane is crucial for its function.

Our study has several limitations that should be considered when interpreting the results. First, all experiments were conducted in a single animal model (*db/db* mice). Although this model replicates key features of human DR, including hyperglycemia, retinal thinning, and gliosis, it does not fully capture the complexity of human disease progression. Second, our mechanistic conclusions are based entirely on *in vivo* tissue analyses. The absence of *in vitro* studies using primary Müller cells or Müller cell lines limits our ability to establish direct causality among ChemR23 activation, PTEN function, and AKT phosphorylation. Third, we did not include a *db/db* + SF1670-only treatment group, which makes it difficult to fully separate the PTEN-independent effects of SF1670 from those specifically interfering with ChemR23 signaling. Fourth, although we focused on Müller cells and RGCs, DR affects multiple retinal cell types, including photoreceptors, bipolar cells, and microglia. Whether ChemR23 activation also influences these cells remains an open question and warrants further investigation. Finally, our study lacks genetic evidence, such as Müller-cell-specific knockout of ChemR23, which would provide stronger support for the cell-autonomous role of ChemR23 in DR pathogenesis.

Conclusions

In conclusion, our study reveals that ChemR23 may regulate AKT phosphorylation through its interaction with PTEN, thereby protecting retinal neurons and suppressing inflammatory responses and Müller cell activation in DR. This suggests novel molecular strategies for treating DR.

Ethical statements

The animal experiments were performed according to the protocols approved by the Ethical Committee of Animal Research at Jinzhou Medical University (No. 2023040201; dated April 2, 2023), and all efforts were made to minimize the number of animals used and their suffering.

Author contributions

The authors confirm their contributions to the paper as follows: experiments, data collection and manuscript writing: Lv T; experimental assistance, testing and theoretical support: Sun S; manuscript revision and financial support: Zuo Z, Feng C. The authors vouch for the accuracy and completeness of the experiment. All authors reviewed the results and approved the final version of the manuscript.

Data availability

All relevant data generated or analyzed during this study are included in this published article.

Acknowledgments

The study was partly financially supported by the Foundation of Education Department of Liaoning Province of China (LJKMZ20221241), the Natural Science Foundation of Liaoning Province of China (2023-MS-312), and the Foundation of Education Department of Liaoning Province of China (JYTMS20231732).

Conflict of interest

The authors declare that they have no conflict of interest.

Dates

Received 14 November 2025; Revised 13 January 2026; Accepted 9 February 2026; Published online 11 May 2026

References

[1] Tan TE, Wong TY. 2023. Diabetic retinopathy: looking forward to 2030. *Frontiers in Endocrinology* 13:1077669
[2] Tomkins-Netzer O, Niederer R, Lightman S. 2024. The role of statins in diabetic retinopathy. *Trends in Cardiovascular Medicine* 34(2):128–135
[3] Pan Z, Zhao Y, Zhou S, Wang J, Fan F. 2023. CD44 drives M1 macrophage polarization in diabetic retinopathy. *Current Eye Research* 48(8):770–780
[4] He S, Gu C, Su T, Qiu Q. 2022. Research progress of circRNAs in inflammatory mechanisms of diabetic retinopathy: an emerging star with potential therapeutic targets. *Current Eye Research* 47(2):165–178
[5] Andrés-Blasco I, Gallego-Martínez A, Machado X, Cruz-Espinosa J, Di Lauro S, et al. 2023. Oxidative stress, inflammatory, angiogenic, and apoptotic molecules in proliferative diabetic retinopathy and diabetic macular edema patients. *International Journal of Molecular Sciences* 24(9):8227
[6] Chen YT, Radke NV, Amarasekera S, Park DH, Chen N, et al. 2025. Updates on medical and surgical managements of diabetic retinopathy and maculopathy. *Asia-Pacific Journal of Ophthalmology* 14(2):100180
[7] Lai D, Wu Y, Shao C, Qiu Q. 2023. The role of Müller cells in diabetic macular edema. *Investigative Opthalmology & Visual Science* 64(10):8
[8] Kumari N, Barman S, Ganesan SK. 2025. Crosstalk between neuronal and glial cells in diabetic retinopathy: mechanisms and implications for neurodegeneration. *Molecular Neurobiology* 63(1):173
[9] Li Y, Zhu L, Cai MX, Wang ZL, Zhuang M, et al. 2023. TGR5 supresses cGAS/STING pathway by inhibiting GRP75-mediated endoplasmic reticulum-mitochondrial coupling in diabetic retinopathy. *Cell Death & Disease* 14(9):583
[10] Li Q, Cheng Y, Zhang S, Sun X, Wu J. 2021. TRPV4-induced Müller cell gliosis and TNF-α elevation-mediated retinal ganglion cell apoptosis in glaucomatous rats via JAK2/STAT3/NF-κB pathway. *Journal of Neuroinflammation* 18(1):271
[11] Zwanzig A, Meng J, Müller H, Bürger S, Schmidt M, et al. 2021. Neuroprotective effects of glial mediators in interactions between retinal neurons and Müller cells. *Experimental Eye Research* 209:108689
[12] Inada M, Xu H, Takeuchi M, Ito M, Chen M. 2021. Microglia increase tight-junction permeability in coordination with Müller cells under hypoxic condition in an in vitro model of inner blood-retinal barrier. *Experimental Eye Research* 205:108490
[13] Rolev KD, Shu XS, Ying Y. 2021. Targeted pharmacotherapy against neurodegeneration and neuroinflammation in early diabetic retinopathy. *Neuropharmacology* 187:108498
[14] Zhang Y, Xu N, Ding Y, Zhang Y, Li Q, et al. 2018. Chemerin suppresses neuroinflammation and improves neurological recovery via CaMKK2/AMPK/Nrf2 pathway after germinal matrix hemorrhage in neonatal rats. *Brain, Behavior, and Immunity* 70:179–193
[15] Zhang Y, Xu N, Ding Y, Doycheva DM, Zhang Y, et al. 2019. RETRACTED ARTICLE: chemerin reverses neurological impairments and ameliorates neuronal apoptosis through ChemR23/CAMKK2/AMPK pathway in neonatal hypoxic-ischemic encephalopathy. *Cell Death & Disease* 10(2):97
[16] Zhang H, Lin A, Gong P, Chen Y, Ye RD, et al. 2020. The chemokine-like receptor 1 deficiency improves cognitive deficits of AD mice and attenuates tau hyperphosphorylation via regulating tau seeding. *The Journal of Neuroscience* 40(36):6991–7007
[17] Corrêa GF, Martins NS, Cipriano UG, Gembre AF, Rodrigues D, et al. 2025. Chemerin exacerbates pulmonary inflammation in type 2 diabetes and *Mycobacterium Tuberculosis* infection comorbidity. *Inflammation* 48(6):4517–4532
[18] Li J, Song L, Song H. 2021. Chemerin promotes microangiopathy in diabetic retinopathy via activation of ChemR23 in rat primary microvascular endothelial cells. *Molecular Vision* 27:575–587
[19] Bäck M. 2023. Icosapent ethyl in cardiovascular prevention: resolution of inflammation through the eicosapentaenoic acid - resolvin E1 - ChemR23 axis. *Pharmacology & Therapeutics* 247:108439
[20] Su X, Cheng Y, Zhang G, Wang B. 2021. Chemerin in inflammatory diseases. *Clinica Chimica Acta* 517:41–47
[21] Zhang J, Yin Z, Xu Y, Wei C, Peng S, et al. 2023. Resolvin E1/ChemR23 protects against hypertension and vascular remodeling in angiotensin II-induced hypertensive mice. *Hypertension* 80(12):2650–2664
[22] Salas-Hernández A, Espinoza-Pérez C, Vivar R, Espitia-Corredor J, Lillo J, et al. 2021. Resolvin D1 and E1 promote resolution of inflammation in rat cardiac fibroblast in vitro. *Molecular Biology Reports* 48(1):57–66
[23] Xie Y, Liu L. 2022. Role of Chemerin/ChemR23 axis as an emerging therapeutic perspective on obesity-related vascular dysfunction. *Journal of Translational Medicine* 20(1):141
[24] Liu L, Zhang J, Lu K, Zhang Y, Xu X, et al. 2024. ChemR23 signaling ameliorates brain injury via inhibiting NLRP3 inflammasome-mediated neuronal pyroptosis in ischemic stroke. *Journal of Translational Medicine* 22(1):23
[25] Suzuki H, Otsuka T, Hitora-Imamura N, Ishimura K, Fukuda H, et al. 2021. Resolvin E1 attenuates chronic pain-induced depression-like behavior in mice: possible involvement of chemerin receptor ChemR23. *Biological and Pharmaceutical Bulletin* 44(10):1548–1550
[26] Zhang Y, Zhang J, Zhao Y, Zhang Y, Liu L, et al. 2023. ChemR23 activation attenuates cognitive impairment in chronic cerebral hypoperfusion by inhibiting NLRP3 inflammasome-induced neuronal pyroptosis. *Cell Death & Disease* 14(11):721
[27] Grewal AK, Singh N, Singh TG. 2019. Neuroprotective effect of pharmacological postconditioning on cerebral ischaemia–reperfusion-induced injury in mice. *Journal of Pharmacy and Pharmacology* 71(6):956–970
[28] Laffranchi M, Schioppa T, Sozio F, Piserà A, Tiberio L, et al. 2025. Chemerin in immunity. *Journal of Leukocyte Biology* 117(3):qiae181
[29] Jin Z, Li G, He D, Chen J, Zhang Y, et al. 2025. An overview of small-molecule agents for the treatment of psoriasis. *Bioorganic & Medicinal Chemistry* 119:118067
[30] Shang J, Wang L, Zhang Y, Zhang S, Ning L, et al. 2019. Chemerin/ChemR23 axis promotes inflammation of glomerular endothelial cells in diabetic nephropathy. *Journal of Cellular and Molecular Medicine* 23(5):3417–3428
[31] Zhang X, Weiß T, Cheng MH, Chen S, Ambrosius CK, et al. 2023. Structural basis of CMKLR1 signaling induced by chemerin9. *bioRxiv* 544295
[32] Zhang J, Liu L, Zhang Y, Yuan Y, Miao Z, et al. 2022. ChemR23 signaling ameliorates cognitive impairments in diabetic mice via dampening oxidative stress and NLRP3 inflammasome activation. *Redox Biology* 58:102554
[33] Yang Q, Lin X, Xiao J, Zhong W, Wang F, et al. 2023. Expression of α-Synuclein in the mouse retina is confined to inhibitory presynaptic elements. *Journal of Comparative Neurology* 531(10):1057–1079
[34] Rangasamy S, Monickaraj F, Legendre C, Cabrera AP, Llaci L, et al. 2020. Transcriptomics analysis of pericytes from retinas of diabetic animals reveals novel genes and molecular pathways relevant to blood-retinal barrier alterations in diabetic retinopathy. *Experimental Eye Research* 195:108043
[35] Ramos H, Bogdanov P, Sabater D, Huerta J, Valeri M, et al. 2021. Neuromodulation induced by sitagliptin: a new strategy for treating diabetic retinopathy. *Biomedicines* 9(12):1772
[36] Orhan C, Tuzcu M, Gencoglu H, Sahin E, Sahin N, et al. 2021. Different doses of β-cryptoxanthin may secure the retina from photooxidative injury resulted from common LED sources. *Oxidative Medicine and Cellular Longevity* 2021:6672525
[37] Mohammad HMF, Sami MM, Makary S, Toraih EA, Mohamed AO, et al. 2019. Neuroprotective effect of levetiracetam in mouse diabetic retinopathy: effect on glucose transporter-1 and GAP43 expression. *Life Sciences* 232:116588
[38] Sanchez MC, Chiabrando GA. 2022. Multitarget activities of Müller glial cells and low-density lipoprotein receptor-related protein 1 in proliferative retinopathies. *ASN Neuro* 14:17590914221136365
[39] Carpi-Santos R, de Melo Reis RA, Gomes FCA, Calaza KC. 2022. Contribution of Müller cells in the diabetic retinopathy development: focus on oxidative stress and inflammation. *Antioxidants* 11(4):617
[40] Du X, Yang L, Kong L, Sun Y, Shen K, et al. 2022. Metabolomics of various samples advancing biomarker discovery and pathogenesis elucidation for diabetic retinopathy. *Frontiers in Endocrinology* 13:1037164

[41] Lu Z, Fan B, Li Y, Zhang Y. 2023. RAGE plays key role in diabetic retinopathy: a review. *BioMedical Engineering OnLine* 22(1):128

[42] Li JJ, Yin HK, Guan DX, Zhao JS, Feng YX, et al. 2018. Chemerin suppresses hepatocellular carcinoma metastasis through CMKLR1-PTEN-Akt axis. *British Journal of Cancer* 118(10):1337–1348

[43] Rennier K, Shin WJ, Krug E, Virdi G, Pachynski RK. 2020. Chemerin reactivates PTEN and suppresses PD-L1 in tumor cells via modulation of a novel CMKLR1-mediated signaling cascade. *Clinical Cancer Research* 26(18):5019–5035

[44] Ben Dhaou C, Mandi K, Frye M, Acheampong A, Radi A, et al. 2022. Chemerin regulates normal angiogenesis and hypoxia-driven neovascularization. *Angiogenesis* 25(2):159–179

[45] Jing Y, Zhang Y, Wang X, Wang Y, Hu Y, et al. 2025. MBD2 promotes B cell differentiation and BCR signaling in systemic lupus erythematosus by regulating the LEF-1-PTEN-PI3K axis. *Cell Death & Disease* 16(1):433

[46] Liu BH, Tu Y, Ni GX, Yan J, Yue L, et al. 2021. Total flavones of *Abelmoschus manihot* ameliorates podocyte pyroptosis and injury in high glucose conditions by targeting METTL3-dependent m^6A modification-mediated NLRP3-inflammasome activation and PTEN/PI3K/Akt signaling. *Frontiers in Pharmacology* 12:667644

[47] Li J, Chen K, Li X, Zhang X, Zhang L, et al. 2023. Mechanistic insights into the alterations and regulation of the AKT signaling pathway in diabetic retinopathy. *Cell Death Discovery* 9(1):418